JOURNAL OF MATERIALS SCIENCE 28 (1993) 3945–3950

Crystal growth and magnetic characterization of $Zn_{1-x}Mn_xCr_2O_4$ single crystals

F. LECCABUE, B. E. WATTS
MASPEC/CNR Institute, Via Chiavari 18/a, 43100 Parma, Italy

D. FIORANI, A. M. TESTA
ITSE/CNR, Area della Ricerca di Roma, P.O. Box 10, 00016 Monterotondo Stazione, Italy

J. ALVAREZ, V. SAGREDO
Departamento de Física, Universidad de Los Andes, Merida, Venezuela

G. BOCELLI
Centro di Studio per la Strutturistica Diffrattometrica/CNR, V.le delle Scienze, 43100 Parma, Italy

Single crystals of $Zn_{1-x}Mn_xCr_2O_4$, where $x = 0$–1, were grown by the chemical vapour transport (CVT) technique using chlorine as the transport agent. A thermodynamic study of both systems, $(ZnCr_2O_4 + MnCr_2O_4)$–Cl_2 and $Zn_{1-x}Mn_xCr_2O_4$–Cl_2, was done in order to investigate the effect of spurious species, i.e. $MnCl_{2(liq)}$, on the transport of the mixed spinel, and structural investigations using X-ray diffraction were carried out. Susceptibility measurements as a function of temperature from 2–300 K for the different compositions are reported, and the magnetic phase diagram was determined as a function of composition and temperature.

1. Introduction

The wide range of cation substitutions which can take place on tetrahedral (A) and octahedral (B) sites in the spinel lattice leads to a number of interesting physical properties, especially if the cation is magnetic [1–4]. Different kinds of magnetic order can be found, as well as disordered magnetic states, e.g. re-entrant ferromagnet, spin-glass. The latter can occur in the presence of a disordered cation occupancy (due to a distribution between A and B sublattices [5], as well as to a disordered substitution in one of the two sublattices [6]) and of magnetic frustration, or due to coexisting ferro- and antiferromagnetic interactions topological in type, in the presence of antiferromagnetic interactions only [7–9].

The system $Zn_{1-x}Mn_xCr_2O_4$ is particularly attractive because competitive antiferromagnetic interactions Cr–Cr, Mn–Cr and Mn–Mn are present [10]. The two normal spinels $MnCr_2O_4$ and $ZnCr_2O_4$ form a solid solution throughout the whole range of composition: $MnCr_2O_4$ is a non-collinear ferrimagnet with $T_C = 43$ K [11] while $ZnCr_2O_4$ orders antiferromagnetically with $T_N = 16$ K [12]. Le Dang *et al.* [11] reported NMR and low a.c. susceptibility of the $Zn_{1-x}Mn_xCr_2O_4$ mixed spinel system and for $x > 0.6$ observed unidirectional anisotropy and remanent magnetization. The existence of a spin-glass state was proposed for a narrow range of compositions.

The details of crystal growth, experimental conditions, as well as the structural characterization have been reported elsewhere [13]. Here, the magnetic properties of the mixed spinel are described in detail. In addition, the thermodynamics of the crystal growth process has been further developed to include the transport of the mixed compound using a model which takes into consideration the presence of $MnCl_2$ as a spurious liquid species.

2. Crystal growth

The polycrystalline spinels $MnCr_2O_4$ and solid solutions $Zn_{1-x}Mn_xCr_2O_4$ (where $0 \leq x < 1$) were sealed in a previously evacuated (10^{-6} torr; 1 torr = 133.322 Pa) quartz ampoule under a chlorine pressure of 0.45 atm at room temperature. Crystal growth was carried out using an average temperature of 990 °C [13].

Fig. 1a and b show some single crystals of $Zn_{1-x}Mn_xCr_2O_4$ with nominal composition $x = 0.3$ and 0.9, respectively. In Fig. 1b it is possible to see a large number of hexagonal platelets of Cr_2O_3. These could be explained by the fact that manganese condenses as $MnCl_2$ and the excess chromium crystallizes as Cr_2O_3.

Single-crystal diffractometry was carried out on a CAD4 or Siemens AED single-crystal diffractometer using MoK_α radiation ($\lambda = 0.071\,069$ nm). The atomic arrangement determined is characteristic of spinels with zinc and manganese atoms occupying the same tetrahedral sites and chromium atoms the octahedral ones. In this disposition, each zinc or manganese is tetrahedrally coordinated while chromium is octahe-

0022–2461

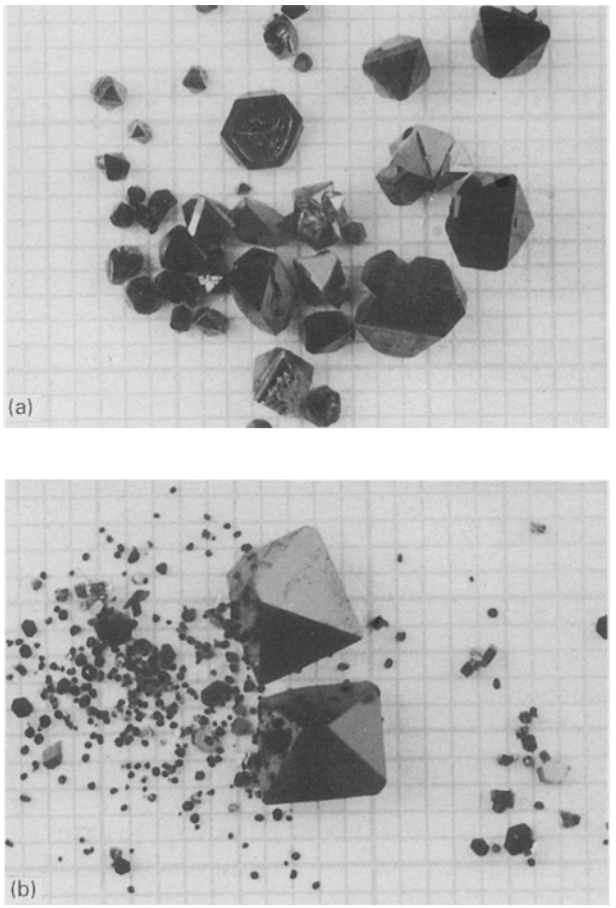

Figure 1 Some single crystals of $Zn_{1-x}Mn_xCr_2O_4$ with composition: (a) $x = 0.3$, and (b) $x = 0.9$. Note the presence of a large number of hexagonal platelets of Cr_2O_3.

drally coordinated with oxygen. It has been shown [13] that the cell parameter increased linearly with nominal manganese content. For the composition $x = 0.7$, the crystal was depleted in manganese with respect to the original powder and this was explained by the formation of the liquid phase.

2.1. Thermodynamic analysis

The $ZnCr_2O_4$–Cl_2 [14] and $MnCr_2O_4$–Cl_2 [13] systems have already been studied and in this work the thermodynamic system has been further refined to include the $Zn_{1-x}Mn_xCr_2O_4$ mixed spinel. Moreover, a calculation was made for a system with two separate spinel phases; the zinc and manganese may have different reactivities with the chlorine and the transport reaction may not follow the stoichiometric ratios of the solid solution.

The gaseous species considered were Cl_2, O_2, $MnCl_2$, $ZnCl_2$, Zn_2Cl_4, $CrCl_2$, $CrCl_3$, $CrCl_4$, CrO_2Cl_2.

Two possible reactions of chlorine with the solid phases are described below.

(a) With $Zn_{1-x}Mn_xCr_2O_4$ giving an equilibrium

$$Zn_{1-x}Mn_xCr_2O_4 + 3Cl_2 \rightarrow (1-x)\,ZnCl_2(g) + xMnCl_2(g) + 2CrCl_2 + 2O_2 \quad (1)$$

The stoichiometric constraints on this reaction are

$$P_{O_2} = P_{CrCl_2} + P_{CrCl_3} + P_{CrCl_4} \quad (2)$$

$$P_{O_2} + P_{CrO_2Cl_2} = 2[P_{ZnCl_2} + 2P_{Zn_2Cl_4} + P_{MnCl_2}] + (RT/V)n_{MnCl_2} \quad (3)$$

$$x[P_{ZnCl_2} + 2P_{Zn_2Cl_4}] = (1-x)[P_{MnCl_2} + (RT/V)n_{MnCl_2}] \quad (4)$$

where P_i ($i = Cl_2$, O_2, etc) are the respective partial pressures of the nine gaseous species present in the system, n_{MnCl_2} is the number of moles of $MnCl_2$ liquid formed in the ampoule, and V the volume of the ampoule.

(b) With ($ZnCr_2O_4 + MnCr_2O_4$) giving equilibria

$$ZnCr_2O_4(s) + 3Cl_2 \rightarrow ZnCl_2(g) + 2CrCl_2 + 2O_2 \quad (5)$$

$$MnCr_2O_4(s) + 3Cl_2 \rightarrow MnCl_2(g) + 2CrCl_2 + 2O_2 \quad (6)$$

The stoichiometric constraints on these reactions are

$$P_{O_2} = P_{CrCl_2} + P_{CrCl_3} + P_{CrCl_4} \quad (7)$$

$$P_{O_2} + P_{CrO_2Cl_2} = 2[P_{ZnCl_2} + 2P_{Zn_2Cl_4} + P_{MnCl_2}] + (RT/V)n_{MnCl_2} \quad (8)$$

In addition there is an equation which conserves the total number of moles of chlorine in the systems, n_{Cl_2}

$$n_{Cl_2} = (V/RT)(P_{Cl_2} + P_{MnCl_2} + P_{CrCl_2} + P_{CrO_2Cl_2} + 1.5P_{CrCl_3} + 2P_{CrCl_4} + 2P_{Cr_2Cl_4}) + n_{MnCl_2} \quad (9)$$

When $MnCl_2$ is present as liquid, an additional equation is needed to solve for n_{MnCl_2}. The vapour pressure of $MnCl_2$ liquid as a function of temperature is given by [15]

$$\log_{10}(P_{MnCl_2}) = -10\,606\ T^{-1} - 4.33\log_{10}(T) + 23.68 \quad (10)$$

where $P_{MnCl_2\,liq}$ is in mm Hg. Table I lists the enthalpy and entropy values used to calculate the vapour pressures.

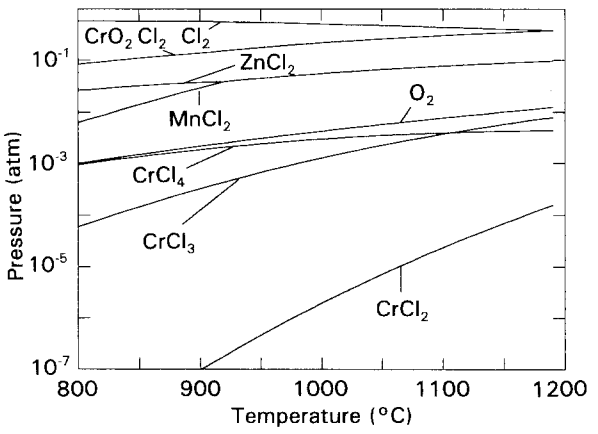

Figure 2 Partial pressures calculated for the $Zn_{0.5}Mn_{0.5}Cr_2O_4$–Cl_2 system as a function of temperature assuming a pressure of Cl_2 of 0.2 atm at 300 K.

TABLE I Thermodynamic data used in the calculations: standard enthalpy of formation, ΔH^0_{298}, entropy, S^0_{298}, and heat capacity, C_p

Compound	ΔH^0_{298} (kcal mol^{-1})	S^0_{298} (e.u.)	$C_p = a + b10^{-3}T + c10^5T^{-2}$ (cal deg^{-1} mole^{-1})			References
			a	b	c	
$ZnCr_2O_4$	− 370.5	29.8	25.5	21.7	0	[16, 17]
$MnCr_2O_4$[a]	− 377.000	33.7	30.0	–	–	[18, 19]
Cl_2	0.000	53.28	8.76	0.27	− 0.65	[18]
O_2	0.0	49.00	8.27	0.25	− 1.877	[18]
$ZnCl_2$	− 63.881	65.091	14.4	0.2	0	[20]
Zn_2Cl_4	− 154.062	98.182	–	–	–	[21]
CrO_2Cl_2	− 128.6	78.8	25.48	0	− 4.75	[18]
$CrCl_2$	− 30.248	74.636	14.004	0	0	[22]
$CrCl_3$	− 78.1	77.0	19.8	0	− 2.6	[23]
$CrCl_4$	− 104.5	84.2	25.46	0.24	− 2.36	[23]
$MnCl_2$	− 70.6	61.671	16.29	− 0.38	− 1.08	[20]

[a] Estimated values.

The partial pressures of the different species as a function of temperature for the transport reaction of $Zn_{0.5}Mn_{0.5}Cr_2O_4$ are plotted in Fig. 2 and for the reaction with ($ZnCr_2O_4$ + $MnCr_2O_4$) in Fig. 3. In both systems the transport is from hot to cold throughout the temperature range considered. Liquid $MnCl_2$ is present below 850° and 1030 °C in the ($ZnCr_2O_4$ + $MnCr_2O_4$) and $Zn_{0.5}Mn_{0.5}Cr_2O_4$ systems, respectively. The presence of a spurious phase may change the zinc to manganese ratio in the crystals from the nominal composition. This was seen [13] to happen for nominal values of $x = 0.7$ and 0.9, while the calculations indicate the presence of liquid for $x = 0.5$. Although there be some uncertainties in the thermodynamic data used, the calculations also suggest that if the transport reaction is not stoichiometric with the nominal composition, the condensation of $MnCl_2$ may be shifted to lower temperatures.

In Fig. 4 the temperature at which $MnCl_2$ liquid condenses is plotted versus initial chlorine filling pressure for the Cl_2–$Zn_{0.5}Mn_{0.5}Cr_2O_4$ system. This curve is a guide to the conditions under which the crystals should be grown, remembering that a suitable compromise must be reached between an acceptable transport rate (high temperature and Cl_2 pressure), avoiding the spurious phase (high temperature and low Cl_2 pressure) and little reaction with the quartz tube (low temperature, low Cl_2 pressure).

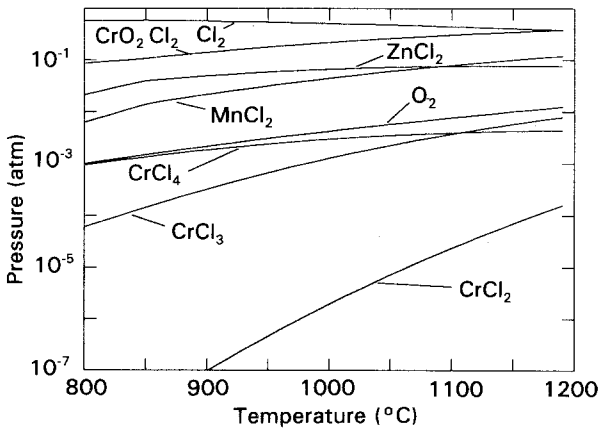

Figure 3 Partial pressure for $ZnCr_2O_4$ + $MnCr_2O_4$ system as a function of temperature assuming a pressure of Cl_2 of 0.2 atm at 300 K.

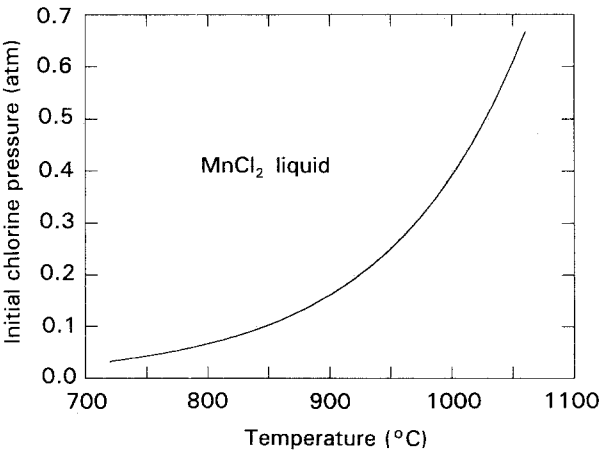

Figure 4 Calculated temperature at which $MnCl_2$ liquid appears versus temperature during the growth of $Zn_{0.5}Mn_{0.5}Cr_2O_4$.

3. Susceptibility measurements

D.c. susceptibility measurements were performed in the temperature range 2–300 K; a Faraday balance with Lewis gradient coils was used between 80 and 300 K. The system was calibrated using an NBS Platinum standard. The applied field was 2.5 kOe. In the low-temperature range (2–70 K) a commercial SQUID magnetometer (Quantum Design, H_{max} = 5.5 T) was used. The measurements, performed on single crystals by applying a field of 20 Oe along the ⟨1 1 1⟩ direction, followed the standard zero field cooling (ZFC) and field cooling (FC) procedures.

The $Zn_{1-x}Mn_xCr_2O_4$ system seems to be particularly attractive because of the coexistence of competitive Cr–Cr (B–B), Mn–Cr (A–B) and Mn–Mn (A–A) antiferromagnetic interactions, the last being weaker than the others. $ZnCr_2O_4$ ($x = 0$) is an antiferromagnet (T_N = 16 K, θ = − 424 K [7]), while $MnCr_2O_4$ is a non-collinear ferrimagnet, T_C = 43 K [6]. The substitution of zinc by manganese ions, progressively changing the spin structure and the resulting magnetic interactions, leads to a magnetic mo-

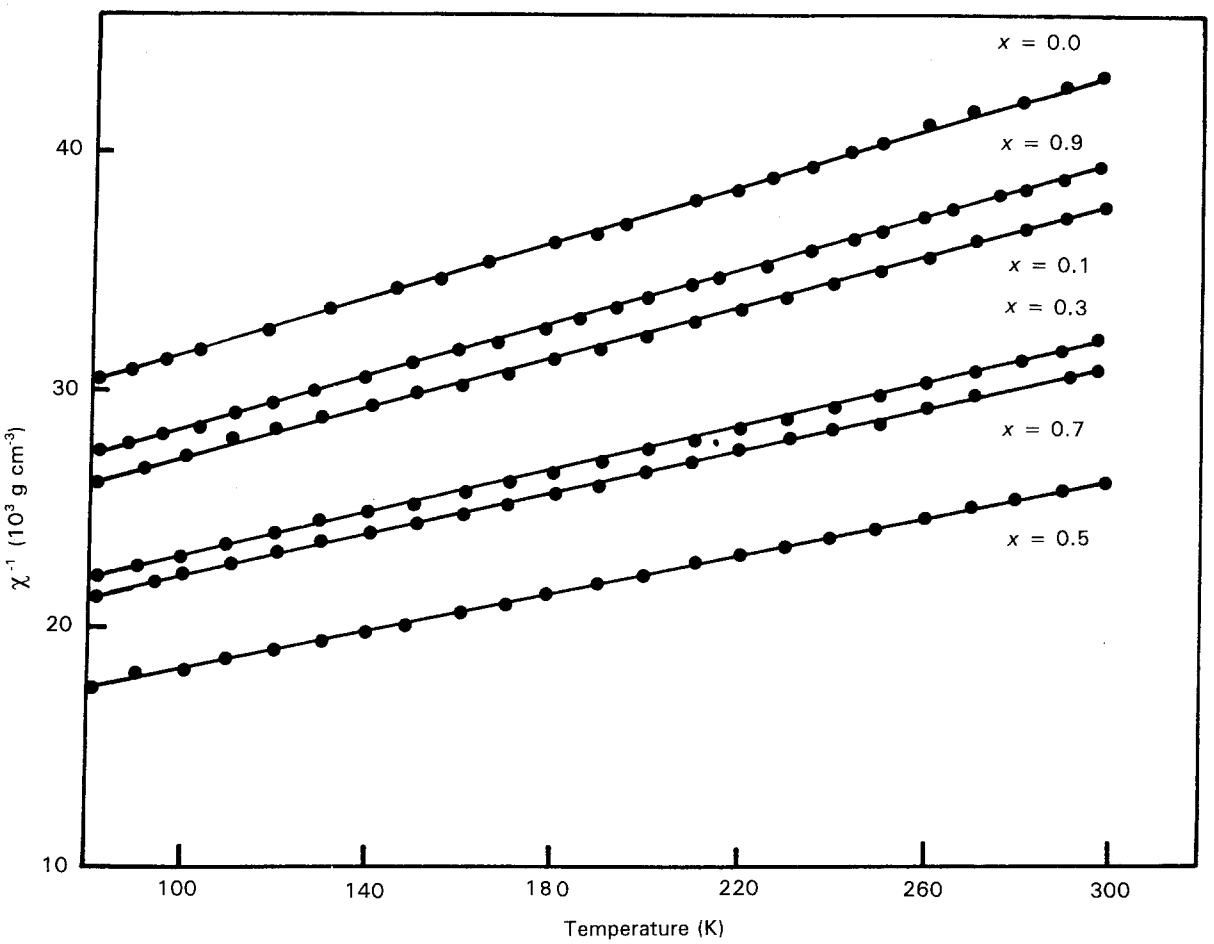

Figure 5 Inverse susceptibility of $Zn_{1-x}Mn_xCr_2O_4$ as a function of the temperature (80–300 K) for different compositions.

ment on the tetrahedral sites. The composition dependence of the effective magnetic moment, μ_{eff}, and of the asymptotic Curie temperature, θ, deduced from the χ^{-1} versus T (K) plots (see Fig. 5) showing a Curie–Weiss behaviour, are reported in Table II.

At a composition $x = 0.5$, magnetic moment shows a maximum and θ a minimum value. The substitution of zinc by manganese ions progressively perturbs the antiferromagnetic structure, leading to a reduction of θ for decreasing x down to $x = 0.5$. At the same time, the effective magnetic moment reaches a maximum for $x = 0.5$; the increase is due to the introduction of the magnetic ion in place of a non-magnetic one. Above $x = 0.5$, θ increases, as long as strong Cr–Mn antiferromagnetic interactions are established, progressively stabilizing the ferrimagnetic structure. The decrease of μ_{eff} is related to the partial compensation of the chromium and manganese magnetic moments, due to the antiferromagnetic interactions.

TABLE II Asymptotic Curie temperature, θ, Curie constant, C, and effective magnetic moment, μ_e, as a function of manganese content

x (Mn)	θ (K)	C (cm^3 mol^{-1} K)	$\mu_e(\mu_B)$
0.0	− 424	0.0166	3.94
0.1	− 414	0.0188	4.09
0.3	− 399	0.0217	4.17
0.5	− 400	0.0225	3.88
0.9	− 403	0.0177	3.31

Low-field and low-temperature susceptibility measurements are reported in Fig. 6. The ZFC branch shows a sharp maximum at T_{max}, the spin-glass freezing temperature, whereas the FC curve continues to increase below T_{max}. Except for $x = 0.3$, the FC and ZFC curves split just below T_{max}. Both the maximum in χ_{ZFC} and the irreversibility below T_{max} resemble a spin-glass behaviour, although in canonical systems χ_{FC} remains constant or shows a small maximum below the freezing temperature. The data are consistent with previous NMR and susceptibility measurements performed in a limited composition range ($x > 0.6$), showing remanence and unidirectional anisotropy after field cooling for samples with $x = 0.70$ and 0.75 [11]. However, further detailed measurements are needed to confirm the existence of this spin-glass state at low temperature. It is well known, in fact, that a system of correlated magnetic clusters can display a similar macroscopic behaviour, due to the blocking of their resulting moments. For $x = 0.3$ the appearance of irreversibility at 70 K gives clear evidence of a progressive blocking of clusters of spins, which should freeze cooperatively at lower temperatures (T_{max}). The magnetic phase diagram, obtained from the dependence of T_{max} on composition x (including T_N and T_C for $x = 0$ and 1, respectively), is reported in Fig. 7. Starting from $x = 0$ and 1, both the antiferromagnetic and ferrimagnetic states are perturbed and then destroyed, leading to a spin-glass like state, or a cluster glass state in the intermediate composition range. The spin-glass like state, or cluster

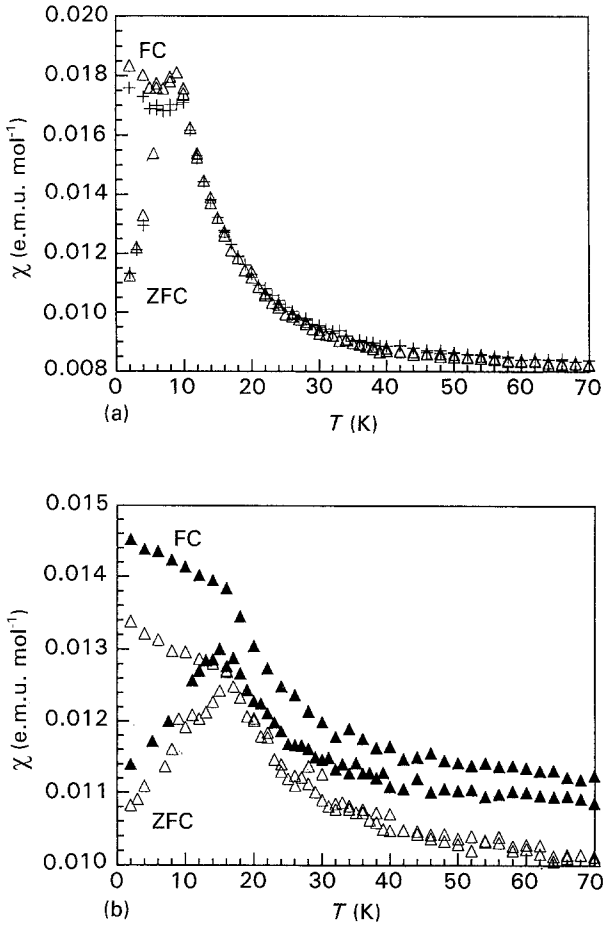

Figure 6 Susceptibility as a function of temperature ($H = 20$ Oe): (a) (△) $x = 0.1$, (+) $x = 0.9$; and (b) (▲) $x = 0.3$, (△) $x = 0.7$.

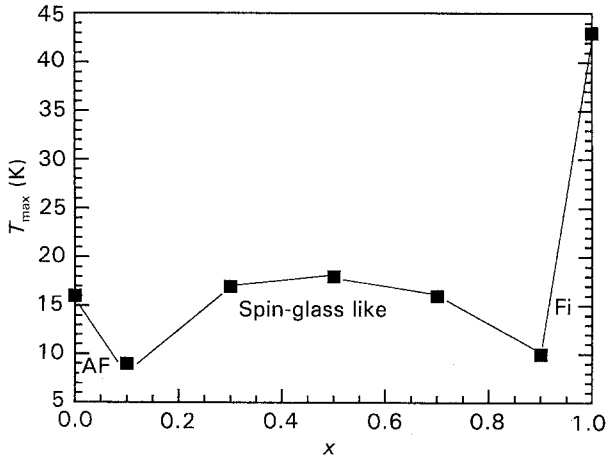

Figure 7 Magnetic phase diagram for $Zn_{1-x}Mn_xCr_2O_4$ in the temperature range 2–300 K (AF = antiferromagnetic, Fi = ferrimagnetic).

glass state characterized by correlated ferrimagnetic regions of different size, are a result of the increased frustration determined by the coexistence of antiferromagnetic interactions competing between them. The existence of ferrimagnetic domains, with a structure similar to that of $MnCr_2O_4$, was detected by NMR spectra for the composition $x = 0.7$ [11]. This is consistent with a cluster-glass picture.

4. Conclusion

Pure and mixed single crystals of $Zn_{1-x}Mn_xCr_2O_4$ spinel with $0 \leq x \leq 1$ have been grown by chemical vapour transport using chlorine as a transport agent. Crystal sizes were typically 2 mm on edge. The crystals with nominal manganese composition $x = 0.7$ were found to be depleted in manganese. A thermodynamic analysis on the $Zn_{0.5}Mn_{0.5}Cr_2O_4$ confirms that liquid $MnCl_2$ would condense causing this depletion. A further analysis treating the system as two separate oxides suggests that the zinc is more reactive with chlorine shifting the range of compositions for which liquid $MnCl_2$ forms to higher values of x.

From susceptibility measurements a magnetic phase diagram (temperature versus composition) was determined, showing the evolution from the antiferromagnetic ($x = 0$) and ferrimagnetic ($x = 1$) state to a spin-glass like state. This could be stabilized by the disordered substitution between zinc and manganese ions in the tetrahedral sublattice, and by the coexistence of different antiferromagnetic interactions, in competition between them.

Acknowledgements

The authors thank Mr R. Panizzieri for his technical assistance, and the CDCH for financial support from projects C-384, C-358 and C-440, and the agreement between CNR/CONICIT.

References

1. E. AGOSTINELLI, F. FILACI, D. FIORANI and A. M. TESTA, *J. Phys. (France)* **C-8**, suppl. 2 (1988) 1061.
2. F. KROK-KOWALSKI, J. WARCZEWSKI and T. MYDLARZ, *ibid.* **C-8**, suppl. 2 (1988) 881.
3. M. GOGOLOWICZ, S. JUSZCZYK, J. WARCZEWSKI and T. MYDLARZ, *Phys. Rev. (B)* **35** (1987) 7073.
4. D. FIORANI and S. VITICOLI, *J. Magn. Magn. Mater.* **49** (1985) 83.
5. J. L. SOUBEYROUX, D. FIORANI, E. AGOSTINELLI, S. C. BHARGAVA and J. L. DORMANN, *J. Phys.* (France) **C-8** 49 (1988) 1117.
6. M. NOGUES, D. FIORANI, J. TEJADA, J. L. DORMANN, S. SAYOURI, A. M. TESTA and E. AGOSTINELLI, *J. Magn. Magn. Mater.* **104–107** (1992) 1641.
7. J. VILLAIN, *Z. Phys. B* **33** (1979) 31.
8. D. FIORANI, J. L. DORMANN, J. L. THOLENCE and J. L. SOUBEYROUX, *J. Phys. (France)* **C-18** (1980) 3053.
9. E. VINCENT and J. HAMMANN, *ibid.* **20** (1987) 2659.
10. D. H. LYONS, T. A. KAPLAN, K. DWIGHT and N. HENYUK, *Phys. Rev.* **126** (1962) 540.
11. K. LE DANG, M. C. MERY and P. VEILLET, *J. Magn. Magn. Mat.* **43** (1984) 161.
12. F. LECCABUE, C. PELOSI, E. AGOSTINELLI, V. FARES, D. FIORANI and E. PAPARAZZO, *J. Crystal Growth* **79** (1986) 410.
13. F. LECCABUE, B. E. WATTS, C. PELOSI, D. FIORANI, A. M. TESTA, A. PAJACZKOWKA, G. BOCELLI and G. CALESTANI, *J. Cryst. Growth* **128** (1993) 859.
14. A. PAJACZKOWSKA, W. PIEKARCZYK, P. PESHEV and A. TOSHEV, *Mater. Res. Bull.* **16** (1981) 1091.
15. O. KUBASCHEWSKI, E. LL. EVANS and C. B. ALCOCK, "Metallurgical Thermochemistry", 4th Edn (Pergamon Press, Oxford, 1967).
16. V. P. Glushko (ed.), "Thermal Constants of Substances", Vol. 8 (Viniti, Moscow, 1974) in Russian.
17. YU. D. TRET'YAKOV, "Solid State Reactions" (Khimiya, Moscow, 1978), in Russian.

18. R. C. Weast (ed.), "Handbook of Chemistry and Physics", 56th Edn (CRC, OH, 1974) D–62.
19. S. KRUPICKA and P. NOVAK, in "Ferromagnetic Materials", Vol. 3, edited by E. P. Wolfarth (North-Holland, Amsterdam, 1982) p. 189.
20. I. BARIN and O. KNACKE, "Thermodynamic Properties of Inorganic Substances", Suppl. (Springer, Berlin, 1973).
21. H. SCHÄFER and U. BINNEWEIS, *Z. Anorg. Allg. Chem.* **410** (1974) 251.
22. I. BARIN, O. KNACKE and O. KUBASCHEWSKI, "Thermodynamic Properties of Inorganic Substances", Suppl. (Springer, Berlin 1977).
23. H. OPPERMANN, *Z. Anorg. Allg. Chem.* **359** (1968) 51.

Received 3 August 1992
and accepted 4 January 1993